KEY FACTORS AFFECTING THE PERMEABILITY MEASUREMENT IN CONTINUOUS FIBER REINFORCEMENTS

M. L. Diallo, R. Gauvin and F. Trochu

Center for Applied Research on Polymers
Mechanical Engineering Department, École Polytechnique de Montréal
P.O. Box 6079, Station "Centre-Ville", Montreal, Que., H3C 3A7, Canada

SUMMARY: Good permeability data are essential to any valuable flow simulation of Liquid Composite Molding Processes. Since there is no standard procedure to do it, every laboratory interested in the subject has developed a set-up and a measuring technique. We have done the same in our laboratory. We conducted experiments for in-plane permeability with various fluid / reinforcement combinations over a range of injection conditions. Testing conditions investigated include the type of fluid, the pressure gradient and the porosity. Measurements in the transient and the saturated mode were done. Fiber architecture was also investigated. It was found that reinforcements having the same structure but manufactured with fibers of different tex have different permeability. It shows that the diameter of the fiber bundles has an effect. We also investigated the pressure gradient. It was found that at high cavity pressure, the permeability computed with the Darcy's law is increased. This increase in permeability may be attributed either to channeling effects due to a geometric change in the preform or compressibility of the fiber preform as the pressure increases. In literature, studies of fabric permeability have employed fluids such as silicon oil, motor oil, corn oil, corn syrup, tap or distilled water, etc. To evaluate the fluid effects, permeability experiments were conducted with four fluids: water diluted corn syrup, Dow 200 silicon oil, HETRON 922 vinyl ester resin and glycerin.

KEYWORDS: Permeability, Liquid Composite Molding, Fabric, Reinforcements, RTM, SRIM, Flow simulation, Preform.

INTRODUCTION

Continuous fiber reinforcement thermoset polymeric composites can be produced by injecting a reactive liquid resin into a mold with preplaced reinforcement. The two best known liquid composite molding (LCM) processes are Resin Transfer Molding (RTM) and Structural Reaction Injection Molding (SRIM). In these processes the reactive liquid is pumped into the mold where fiber reinforcement has been preplaced. After the cure cycle of the injected resin is completed, the mold is opened and the composite part can be removed. Typically, in RTM, resin reactivity is lower than for SRIM and viscosity higher. In these processes, injection pressure could be as low as 0.1 MPa and as high as 3 MPa. In many cases, low cost fiberglass-polyester or epoxy tools are used. In these processes, the reinforcement could take several forms, for instance, it could be a stitched preform, a continuous strand mat or any type of fabrics such as a woven roving, a non-crimp stitched (NCS) fabric, a woven fabric or a combination of two or more of these reinforcements.

In addition to the necessary pressure to compress the reinforcements into the mold, the resin pressure generated during mold filling is an important parameter in mold design and equipment selection. The major variables controlling the resin pressure developed in the mold are the permeability of the fiber reinforcement, viscosity of the resin, and flow rate. The flow rate can be directly controlled by the injection equipment. The viscosities of the resins can be measured by commercially available viscometers. In order to successfully predict the pressure gradients within the mold, accurate permeability data must be available for all reinforcements used. The permeability is also of interest for the prediction of fill times. However a substantial amount of permeability data have appeared in the literature [1-10]. Since there is no standard procedure for permeability measurement, every laboratory interested in the subject has developed a set-up and a measuring technique. Usually, permeability data are obtained from experiments based on Darcy's law. This law states that the macroscopic velocity of the flow is related to the pressure gradients through the following equation:

$$v = \frac{[K]}{\mu} \nabla P \qquad (1)$$

where v is the macroscopic flow velocity, ∇P is the pressure gradient, [K] is the permeability tensor and μ denotes the resin viscosity.

This paper presents the results of an extensive study to evaluate the influence of several parameters on permeability measurement.

EXPERIMENTAL

Reinforcement

Four different reinforcements were used for the tests. These are:

1. JB Martin NCS 81053: a non-crimp, stitch bonded, bi-directional material consisting of high tex fiber bundles and is balanced with 48,9% of its weight in both weft and warp directions. The remainder of its weight 2.2% comprised two stitching polyester threads in the warp layer (1.5%) and a third one (0.7%) in the weft layer. The overall surface density is 618 g/m^2.
2. JB Martin NCS 82675: it has the same weave as the JB 81053 but with lower tex fiber bundles. Its overall fabric weight is 315 g/m^2.
3. Thermoformable glass fabric from Brochier, the EB 315-E01-120, which has an anisotropic permeability and a surface density of 315g/m^2. It is named the Injectex fabric by the company. To facilitate the flow in the weft direction it is stitched with polyester threads allowing high permeability in this direction, the Injectex direction, and a relatively low one in the warp direction. Permeability was measured as received and after thermoforming.
4. Injectex GB 390 E02 -107: a thermoformable balanced carbon fabric from Brochier. Its surface density is 390 g/m^2 .

Schematics of these materials are shown in figure 1.

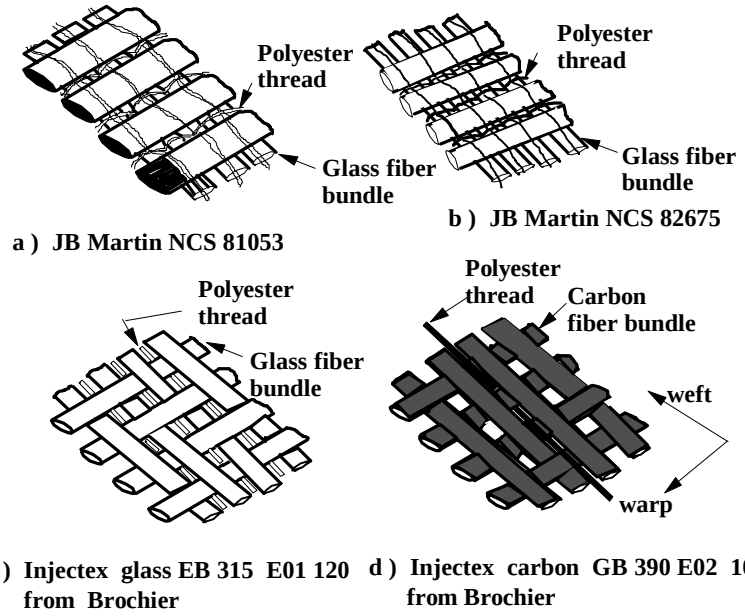

Figure 1. Schematics of the reinforcements used

Test fluids

Four fluids, water diluted corn syrup, Dow 200 silicon oil, HETRON 922 vinyl ester resin and glycerin were used. The viscosities are about 100 centipoise (Cp), 102 Cp, 360 Cp and 865 Cp, respectively. Viscosity at room temperature was measured using a Brookfield LVT-DV1 digital viscometer. Both the corn syrup and the silicon oil are widely used in the literature and their Newtonian behavior is excellent. Also the corn syrup has the advantage to be easy to handle and to wet the glass fabric very well. To ease the flow front visualization, the corn syrup was colored green prior to testing. For a better conservation, 2000 PPM of sodium azide are added to aqueous corn syrup to insure a bactericidal effect.

Apparatus

A rectangular mold filling apparatus is used for unidirectional permeability measurement. The mold assembly is made of two tempered glass plates of 93 cm x 13 cm x 1.9 cm.. Tempered glass is used instead of plexiglass to minimize plaque deflection. The mold cavity is formed with a 2.4 mm thick picture frame. Silicone sealant is used to prevent edge effects. A diaphragm pressure transducer 0 - 500 Kpa is mounted near the inlet port and a constant inlet flow rate is obtained with a cylinder mounted on a tensile testing machine.

Care was taken to remove all air bubbles from the tubing lines before each experiment. The JB Martin NCS reinforcements were sprayed with a very thin line of glue before cutting the specimen from the roll to reduce the fraying of the materials. Initial tests without the glue line showed a very high by-pass flow along the edges due to the reduction in glass volume fraction where the material had frayed.

The necessary precaution was taken to assure a plug flow. Each reinforcement layer was weighed before the experiments. Fiber volume fraction was determined by the following equation:

$$V_f = \frac{n\zeta}{h\rho_f} \qquad (2)$$

where V_f is the volume fiber fraction, n is the number of layers, ζ is the layer surface density, h is the cavity thickness and ρ_f the density of the fiber. The density of fiber is taken from published literature (for E-glass, 2.56 x 10^6 kg/m^3 ; carbon fiber, 1.77 x 10^6 kg/m^3).

RESULTS AND DISCUSSIONS

To measure the transient in-plane permeability, so called dry permeability, the elapsed time t is recorded at every 2 centimeters during the mold filling and the inlet pressure P_0 (t) is also collected. From the experimental data, plot of permeability vs front position is constructed. Example of permeability plot is shown in figure 2. It can be observed that during the first few cm of mold filling, the flow appears to be in transition, and the figure shows that it takes some distance for the flow to stabilize. This results in a higher permeability at the beginning. This phenomenon was observed earlier [10,11] and was mainly attributed to the relative significance of the capillary effects at the beginning of the filling. This lead us to suggest a minimum length for the permeability measurement in a unidirectional flow experiment [12].

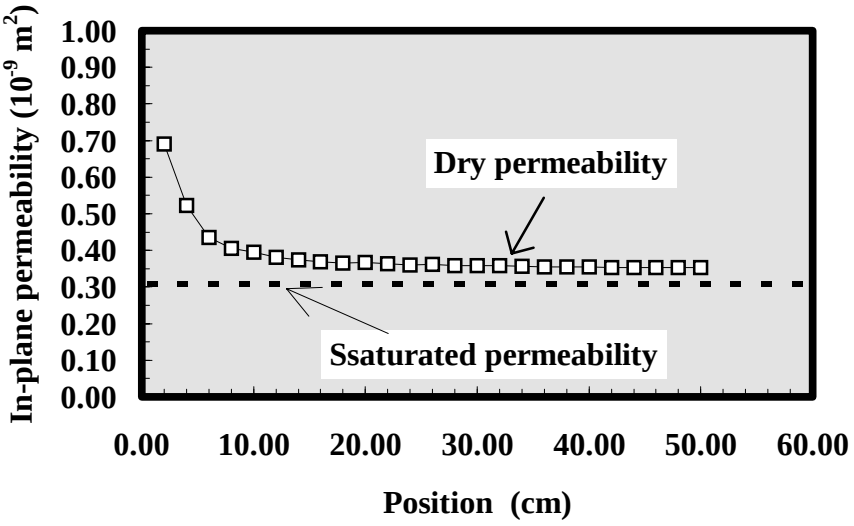

Figure 2. Permeability convergence of a typical run
JB 82675 (weft), V_f =41%

Figure 3 shows the pressure traces during a typical run. As expected, the initial part of the curve is almost linear. As it can be seen, the inlet pressure reaches its maximum after the flow front has exited the reinforcement. While the pressure continues to rise, air bubbles flow out the reinforcement. This steady value corresponds to the pressure used to calculate the saturated permeability. It is worth remembering that Darcy's law is defined for a saturated porous media.

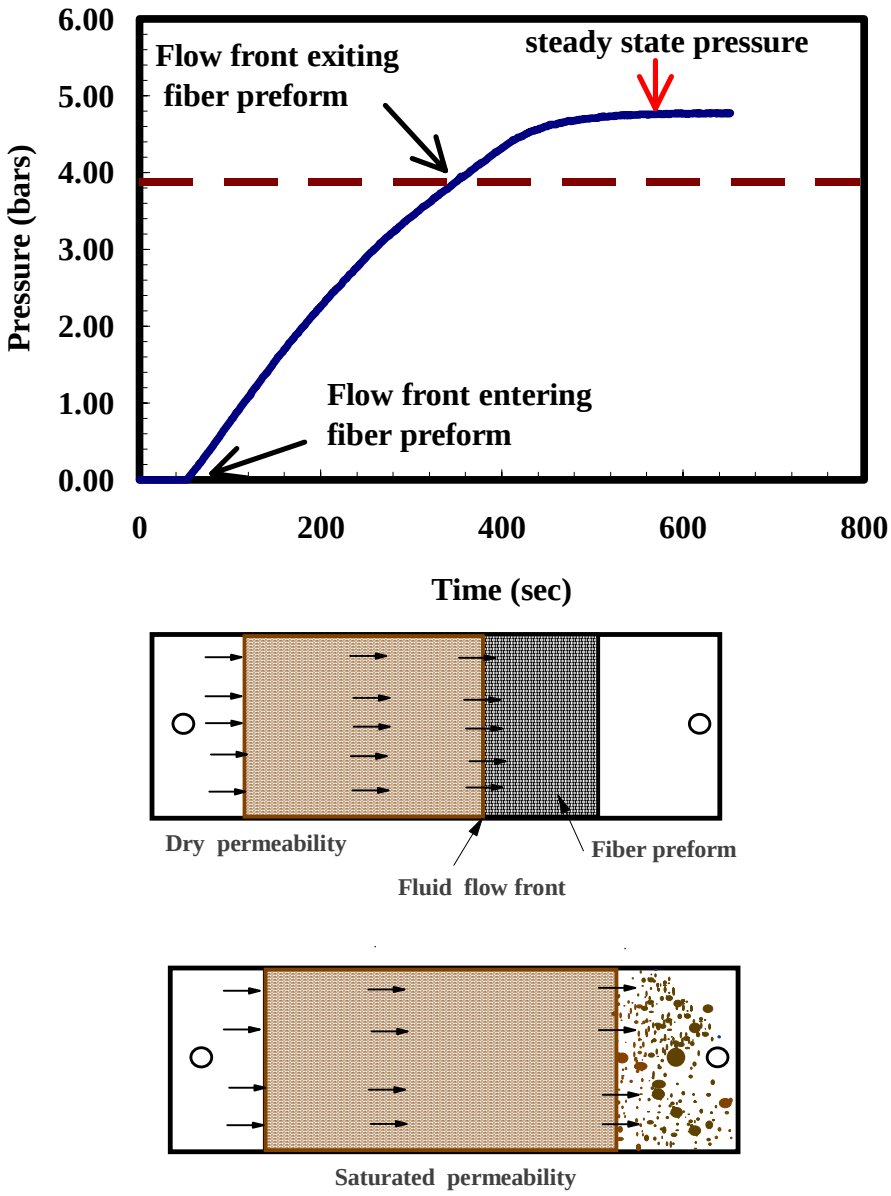

Figure 3. Pressure versus time during filling

A serie of experiments was performed at various fiber volume fractions V_f with the different reinforcements. The permeability of each reinforcement as a function of V_f is presented in figures 4, 5 and 6. One can see on figure 5 that when a preform was used rather than a layered bed, the material permeability was found slightly smaller.

With the carbon fabric, we observed scatter in the permeability values when the permeant fluid is corn syrup (see figure 6). This is probably because the corn syrup does not wet out the carbon fibers well. In fact, a qualitative inspection of the fabric after each permeability experiment revealed that the carbon fiber tows are not evenly wet by the corn syrup.

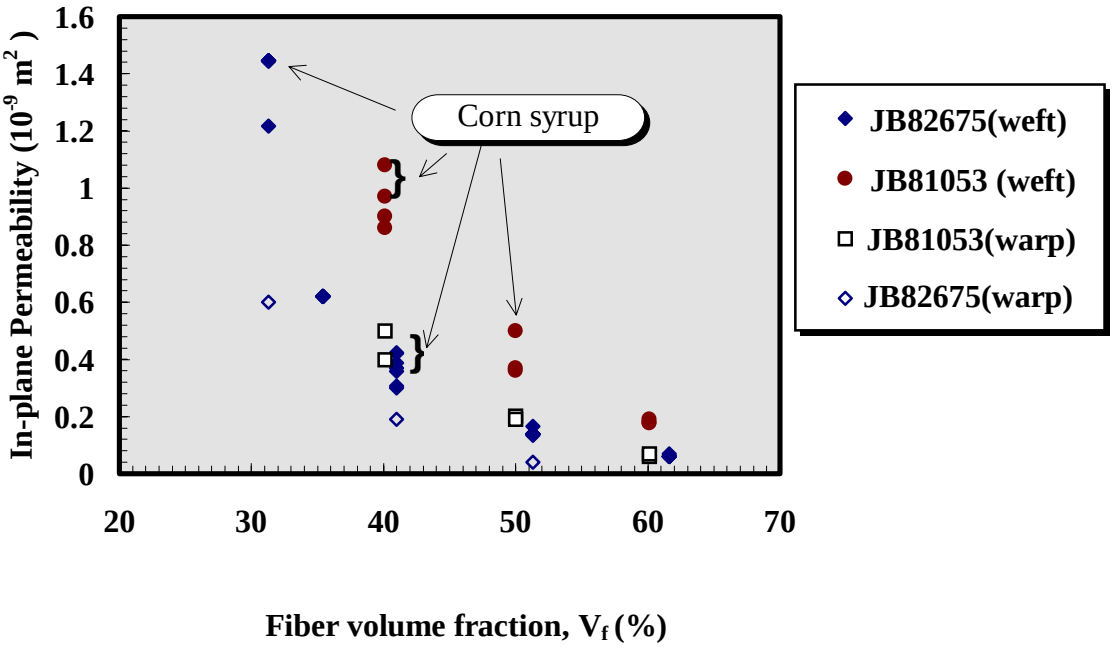

Figure 4. In-plane permeability of JB Martin Non-crimp fabrics. Measurements were done using Dow 200 silicon oil 100 Cst, except for the points indicated otherwise

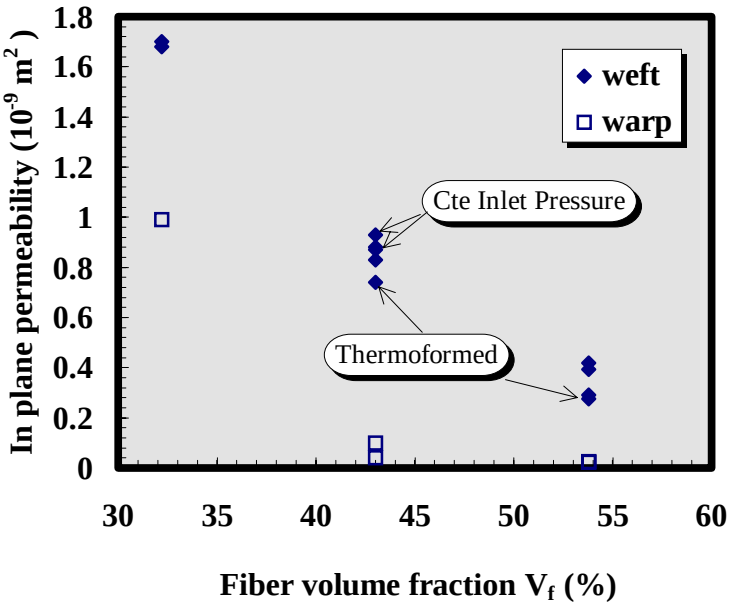

Figure 5. In-plane permeability of Brochier EB 315, obtained using Dow 200 silicon oil 100 Cst. Measurements were done with a constant flow and non thermoformed fabric, except for the points indicated otherwise.

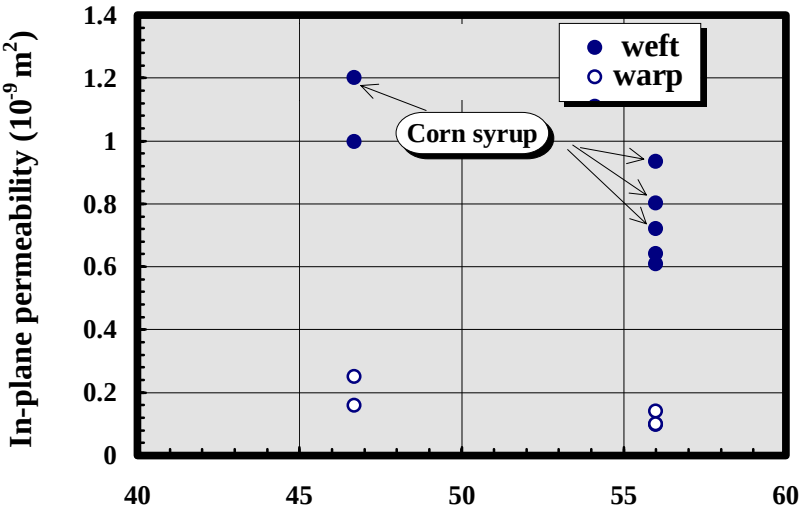

Figure 6. In-plane permeability of Injectex carbon GB 390. Measurements were done using Dow 200 silicon oil 100 Cst, except for the points indicated otherwise

As noted in previous work [13] and by other groups [5, 9, 14], the relationship between permeability and fiber volume fraction is not linear and it can vary significantly. Smaller air bubbles exiting the preform were observed for higher fiber volume fraction. The size and the amount of bubbles were also influenced by the fabric orientation, weft or warp. This phenomenon was also observed by Wang et al. [15] and Carman [16] who mentioned that the size of air bubbles seems to be related to pore structure. We agreed on the influence of pore structure but we should add the pore structure with respect to the flow direction. To study the effect of the air bubbles on the permeability measurement, the fluid was allowed to flow continuously for a certain period of time at a constant flow rate. The air bubbles were flushed out and pressure became steady as indicated above. The permeability was then measured in this saturated regime. It decreased as much as 5 to 10% after complete removal of trapped air.

In our experiments, first the transient permeability is computed point by point with Darcy's law during cavity filling. The value reported here corresponds to the stabilize value as shown in figure 2. Then, with the same sample still sitting in the cavity, the pressure gradient is recorded for each constant flow rate. These experimental points are plot on a graph of (Q/A) versus pressure. The saturated permeability is computed from a least square fit of these data points. An example of such a graph is given in figure 7 for the JB 82675 in the weft direction.

It can be observed that for steady flow experiments, the fabric showed a slight increase in permeability at high pressure gradients. The departure from linearity was also observed by other authors [1,17,18,19,20]. It has been proposed that this effect might be related to fiber movement, which could cause changes in pore structure and result in channeling effect due to higher pressure. Even if a higher pressure increases slightly the saturated permeability, it is always lower than the dry permeability. This is consistent with the experimental results presented in [11,19,21]. One physical explanation for the fact that dry permeability is higher than steady state permeability is provided by consideration of the mechanism by which the air bubbles between adjacent fiber bundles (tows) are displaced as the fluid front advances[22].

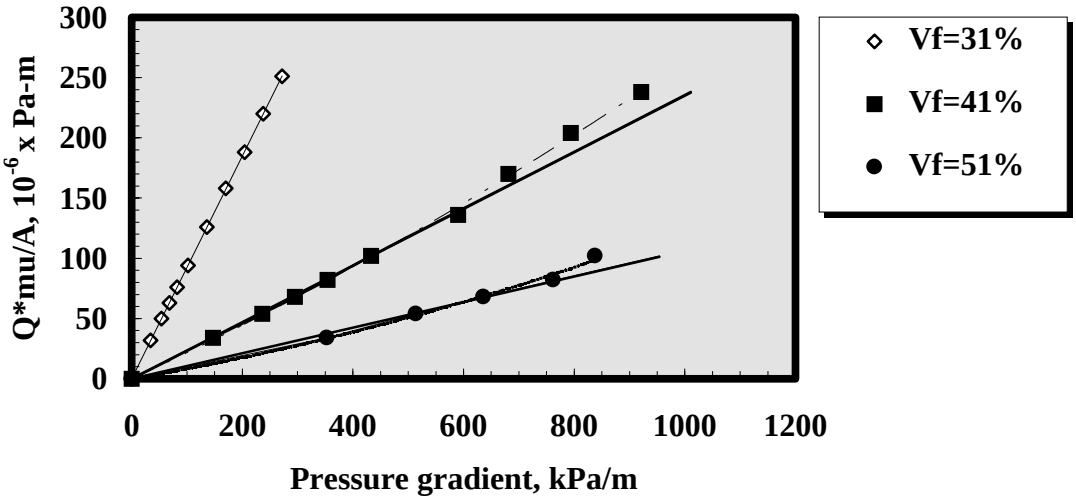

Figure 7. Flow as a function of pressure gradient for the JB 82675 (weft);
μ = 0.102 Pa.s; K_{sat} = 0.924 10^{-9} m^2 (V_f = 31%);*
K_{sat} = 0.235 10^{-9} m^2 (V_f = 41%); K_{sat} = 0.106* 10^{-9} m^2 (V_f = 51%)*

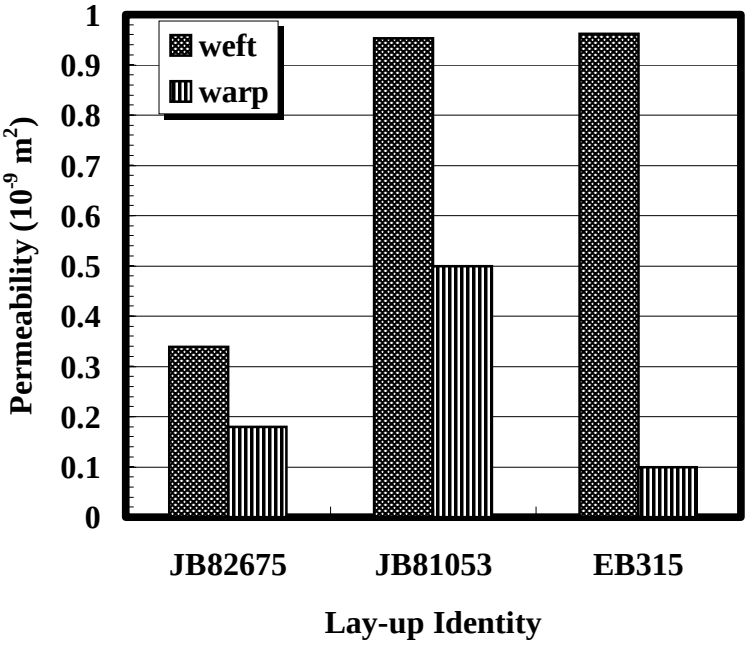

Figure 8. Effect of fiber structure on permeability. $V_f \cong 40\%$.
Values were obtained using Dow 200 silicon oil 100 Cst.

As can be seen in figure 8, the permeability is closely related to fiber architecture and fiber orientation even if the fiber volume fraction is the same. Even if each material investigated had similar tex fibers in both directions, the magnitude of the permeability is much higher in the weft direction. This is attributed to the thread stitches that hold the layers together and run in the weft direction. Both of the JB Martin NCS fabrics had the same architecture but were

manufactured with fiber bundles of different tex. It is likely that the wider fiber tows in the JB 81053 also provide larger inter-tow spaces and hence increase the permeability. The results also indicate that the fiber bundle diameter has an effect on the permeability.

The anisotropy index of the fabrics which is the ratio between the two dry in-plane permeabilities as a function of the fiber volume fraction is given in figure 9. This index is relatively constant for all fabrics tested, except for non thermoformed Brochier EB 315, for which the increase is tremendous.

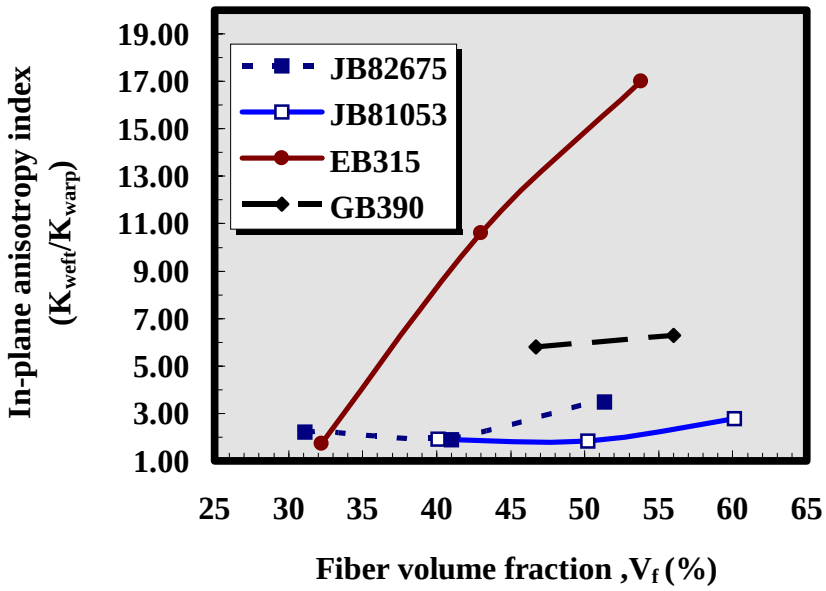

Figure 9. In-plane anisotropy index as a function of fiber fraction V_f

Figure 10 displays the dry in-plane permeability of the non thermoformed Brochier Injectex EB 315 at 41% of fiber volume fraction for the four fluids selected. Furthermore, a non filtered corn syrup was used to see the influence of filtering on permeability. One can see that it is lower with the non filtered corn syrup. Since there are solids in suspension in the non filtered syrup, this results in blocking effects and the computed permeability is reduced. The highest permeability in both directions corresponds to the use of the glycerin and the lowest to the use of non filtered corn syrup.

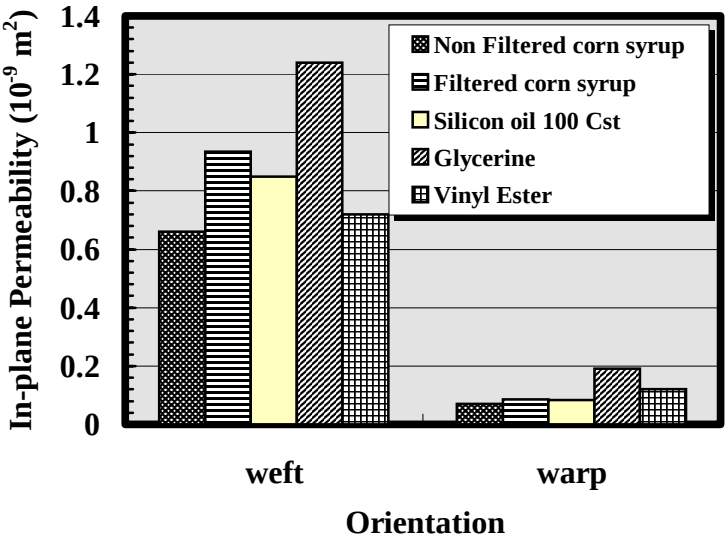

Figure 10. Permeability for non thermoformed Brochier EB 315 as a function of permeant fluid. Fiber volume fraction = 41%

CONCLUSION

Fluid flow through continuous fiber reinforcements has been studied. It was found that in addition to the porosity several other parameters influence the permeability measurement. These parameters include 1) type of fluid, 2) cavity pressure level, 3)fiber structure, and 4) resin saturation. By comparing the results in the wrap and weft directions, it is clearly show that not only the fiber structure or its image, the pore geometry, that influence the permeability but also the orientation of this structure with respect to the flow direction. Also the study shows that there is considerable differences between different types of reinforcement, even at the same fiber volume fraction. Finally, since the fluid can influence significantly the computed permeability, it is advisable to use the resin for the permeability values to be used in simulation code.

ACKNOWLEDGMENTS

The authors would like to thank the NSERC of Canada and the Fond FCAR du Québec for their financial support. The RTMFLOT user's Club members, Aérospatiale, ETH-Zurich, Ford, Matra, Hispano-Suiza, INSA de Toulouse and ISITEM de Nantes are also acknowledged. We also thank J.B. Martin and Armkem for providing free materials.

REFERENCES

1. Kim, Y.R., McCarthy S.P., Fanucci, J.P., Nolet, S.C. and Koppernaes C., 22nd SAMPE Technical Conference, pp.709-723(1990).

2. Hayward, J.S. and Harris, B., Sampe Journal, **26**, 3, pp. 39-46(1990).

3. Steenkamer, D.A., Wilkins, D.J., Karbhari, V.M., J. Mater. Sc. Let., **12**, 971-973(1993).

4. Greve, B. N. and Soh, SAE transaction, **99**, 5, pp. 331-343, 1990.

5. Molnar, J. A. , Trevino, L. and Lee, L. J. , Polym. Compo., **10** , 6, pp.414(1989).

6. Fracchia, C.A., Master thesis, Mech. Eng., Univ. of Illinois, Urbana-Champaign(1990).

7. Verhus, A.S. and Peeters, J.H.A., Compos. Manufact., **4,** 1, pp 33-37(1993).

8. Gauvin, R., Trochu, F., Lemenn, Y. and Diallo, L., Polym. comp., **17**(1):34-42 (1996).

9. Coulter J.P., Smith B. and Guceri S., Proc. of the Am.Soc. for Compo., **2:**209(1987)

10. Luce, T.L., Advani, S.G., Howard, J.G. and Parnas, R.S.,with the permission of the authors, submitted to Polymer Composites.

11. Williams, J.G., Morris, C.E.M. and Ennis, B.C. Poly. Eng. Sci., **14**, 413(1974).

12. Ferland, P. Guittard, D. Trochu, F., Polym. Comp., **17**(1):149-158(1996).

13. Gauvin, R. and Kerachni, A., J.E.C., Août 1992.

14. Cai, Z. Compos. Manufact., **3,** 4, pp 251-257(1992).

15. Wang T.J., Perry M.L. and Lee L. J., Antec, pp.756-760(1992)

16. Carman, P. C., Trans. Am. Inst. Chem. Eng., **15**, 150(1937)

17. Gauvin, R., Chibani, M. and Lafontaine, L., 41st Ann. Conf., Compos. Inst., Soc. Plas. Ind., 19-B(1986).

18. Mishra, S. and Jayaraman, K., SAE, International Congress and Exposition, N.930174, Detroit, Michigan, March 1-5 , 1993.

19. Martin, G. Q., and Son, J. S., ASM Conference on Advanced Composites, **2**, pp. 149(1986)

20. Dave R. and Houle S., Proc. of the Am. Soc. for Compo., **4**, pp. 539(1990).

21. Foley M.F., Gutowski T., 23rd SAMPE Technical Conference, pp.326-340(1991).

22. Parnas, R. S. and Phelan, F. R., SAMPE Q., **22**, 6, pp.53(1991).